Böhling, Daniel; Cwirzen, Andrzej; Habermehl-Cwirzen, Karin

Bond Strength between Glass Fiber Fabrics and Low Water-to-Binder Ratio Mortar

Published in:
Advances in Civil Engineering

DOI:
10.1155/2018/8197039

Published: 02/09/2018

Document Version
Publisher's PDF, also known as Version of record

Hindawi
Advances in Civil Engineering
Volume 2018, Article ID 8197039, 10 pages
https://doi.org/10.1155/2018/8197039

Research Article

Bond Strength between Glass Fiber Fabrics and Low Water-to-Binder Ratio Mortar: Experimental Characterization

Daniel Bohling,[1] Andrzej Cwirzen,[2] and Karin Habermehl-Cwirzen[2]

[1]*Aalto University, Helsinki, Finland*
[2]*Luleå University of Technology, Luleå, Sweden*

Correspondence should be addressed to Andrzej Cwirzen; andrzej.cwirzen@ltu.se

Received 19 February 2018; Revised 27 June 2018; Accepted 2 August 2018; Published 2 September 2018

Academic Editor: Cumaraswamy Vipulanandan

Full utilization of mechanical properties of glass fiber fabric-reinforced cement composites is very limited due to a low bond strength between fibers and the binder matrix. An experimental setup was developed and evaluated to correlate the mortar penetration depth with several key parameters. The studied parameters included fresh mortar properties, compressive and flexural strengths of mortar, the fabric/mortar bond strength, fabric pullout strength, and a single-lap shear strength. Results showed that an average penetration of mortar did not exceed 100 μm even at a higher water-to-binder ratio. The maximum particle size of the used fillers should be below an average spacing of single glass fibers, which in this case was less than 20 μm to avoid the sieving effect, preventing effective penetration. The pullout strength was strongly affected by the penetration depth, while the single-lap shear strength was also additionally affected by the mechanical properties of the mortar.

1. Introduction

One of the early attempts to produce ultrahigh strength concrete (UHPC) was made in the beginning of the 1970s. Very fine Portland cement clinker was mixed with potassium carbonate to control the hydration of calcium aluminates. Lignosulfonate-based plasticizer was used to provide a sufficient workability at the water-to-binder (W/B) ratio of 0.2 [1]. Developed in the 1980s, the so-called DSPs (densified with small particles) concrete utilized a large amount of silica fume, new generation of superplasticizers coupled with strong coarse aggregates [2]. As a result, the 28-day compressive strength exceeded 200 MPa. Another example of the ultrahigh strength concrete is called MDF (Macro Defect Free) [3]. The MDF concrete combined cement with polyvinyl alcohol (PVA) polymers, which acted as a dispersant and a cross-link between aluminate ions. The compressive strength reached 650 MPa. Unfortunately, regression of the strength was observed when the MDF concrete was exposed to water. Currently used ultrahigh strength concrete is derived extensively from the research initiated by De Larrard [4] and his linear packing density model (LPDM), solid suspension model (SSM), and compressive packing model (CPM). Later, Richard and Cheyrezy [5] developed a reactive powder concrete (RPC). Ultrahigh strength is achieved by optimization of the particle-packing density using ultrafine particles coupled with a very low W/B ratio, usage of modern superplasticizers, and application of heat treatment. The UHPC is very fluid in most cases, which makes it theoretically suitable to be combined with textile reinforcement. Textile-reinforced concrete (TRC) is commonly referred to as being a composite made from a fine-grained concrete matrix having the largest aggregate size in the range of 1 mm and continuous reinforcement made from textiles. The used textiles are based on multifilament yarns or high-performance fibers such as alkali-resistant glass, carbon, or aramid. The fabric reinforcement can be aligned in the load direction, and it is used in a wide variety of structures where corrosion resistivity and lower weight compared to a conventional steel reinforcement become particularly beneficial to decrease the overall thickness and the weight of the structure [6, 7].

The biggest challenge in utilizing the full potential of TRC is a limited penetration of the cement paste between the fiber bundles [8, 9]. Therefore, the main objective of the research presented in this paper was to develop a testing procedure suitable for the determination of various parameters related to the bond strength between glass fiber fabrics and mortars with a very low W/B ratio. The study also aimed to correlate effects of the W/B ratio and workability on the penetration depth of mortars in between densely packed glass fiber bundles. Furthermore, selected mechanical properties of the composites including shear strength and pullout forces were investigated and correlated with other measured parameters.

2. Materials and Methods

The sulphate-resistant (SR) cement type CEM I 42.5 N (SR) manufactured by Finnsementti Oy was used, and its properties are given in Table 1. The used fine, high-purity silica fume was a by-product from the zirconium industry. As additional fine fillers, EHK quartz originating from quartzite deposits from Eastern Finland and fine sand (particle diameter of 125 to 600μm) were used (Table 2). The fresh mix workability was adjusted by the polycarboxylate-based superplasticizer produced by BASF, type Glenium ACE 403. The fabric reinforcement was a unidirectional stitched glass fiber fabric produced by Ahlström Glassfibre Oy. The benefit of a unidirectional stitched fabric is the ability to orientate the reinforcement in the preferred direction [10]. Basic properties of the used glass fabric are given in Table 3. The used E-glass is unsuitable for concrete composites due to the known long-term degradation. However, the main research objective was the bond strength at the age of 28 days; therefore, the long-term degradation is insignificant. Four different mix designs were utilized (Table 4). The water-to-binder (W/B) ratio varied from 0.2 to 0.26, while the amount of other ingredients was constant. All mixes were produced using an Ecovac Bredent vacuum mixer. The vacuum was applied to remove the entrapped air from the paste. The mixing procedure consisted of premixing by hand to wet the mix followed by vacuum mixing for 2:00 min at the mixing speed of 290 rpm (rounds per minute). All samples were steam cured for 24 hours starting 48 hours after mixing. The workability was determined using a nonstandardized slump-flow test. In the test, 100 ml of the mix was poured from a height of approximately 10 cm on top of a flat surface covered with a sheet of a regular printing paper marked with circular lines placed at known distances, enabling to determine the slump flow (Figure 1). All specimens were produced using Teflon molds to avoid contamination from a demolding oil. Compressive strength values were determined on specimens having dimensions of $12 \times 12 \times 60\,\text{mm}^3$. Specimens used to test the bond strength and the shear strength had dimensions of $10 \times 25 \times 100\,\text{mm}^3$ (Figure 2). Purpose-built Teflon formwork enabled to place the fabric in the middle of the formwork (Figure 3). The compressive strength, flexural strength, and pullout strength were determined using a Zwick Roell RK 250/50 test rig with a loading speed of 0.35 mm/min. The single-lap shear strength test was performed following recommendation of the EN 14869-2 standard, Structural adhesives - Determination of shear behavior of structural bonds-Part 2: Thick adherents shear test (ISO 11003-2 : 2001, modified). This test method was used to determine the shear behavior of an adhesive in a single-lap joint-bonded assembly when subjected to a tensile force. The specimen dimensions used for the shear strength test are shown in Figure 4 and the used setup in Figure 5. Notches were cut using a diamond saw. For each composite, three test specimens were tested at a testing speed of 1 mm/min. The average shear stress was calculated, following the EN14869-2; once the tensile force F has been applied, the average shear stress in the interface was calculated as

$$\tau = \frac{F}{h * a}, \tag{1}$$

where τ = average shear stress (N/mm^2), F = applied tensile load (N), a = width of the specimen (mm), and h = bond length (mm).

Table 1: Chemical composition and clinker components of SR cement.

Component	(%)
CaO	63.1
SiO_2	20.2
Al_2O_3	2.2
Fe_2	4
MgO	2.0
Na_2O	0.18
K_2O	0.31
Loss on ignition	4.5
C_2S	68
C_3S	13
C_3A	1
C_3AF	13

Table 2: EHK quartz composition and physical properties.

Component	(%)
SiO_2	99.4
Al_2O_3	0.3
K_2O	0.06
Fe_2O_3	0.03
L.O.I.	0.2
Specific gravity (g/cm^3)	2.65
Bulk density (t/m^3)	1.1
Hardness (Mohs)	7
pH (10% w/w)	5.5

Table 3: Properties of the glass fabric.

Description	Value
Linear density (Tex)	2400
Glass type	E
Filament diameter, nominal (μm)	17
Glass density (g/cm^3)	2.54
Fabric weight (g/m^2)	1000

Table 4: Mix proportions during primary tests.

Test mix	Cement		Silica fume	Sand	Quartz fillers	SP (solid + water)	W/C	W/B
	Amount	Type	Amount	(100 μm–600 μm)	EHK	Amount		
PR1	1	SR	0.25	0.6	0.2	0.06	0.26	0.20
PR2	1	SR	0.25	0.6	0.2	0.06	0.28	0.22
PR3	1	SR	0.25	0.6	0.2	0.06	0.31	0.24
PR4	1	SR	0.25	0.6	0.2	0.06	0.33	0.26

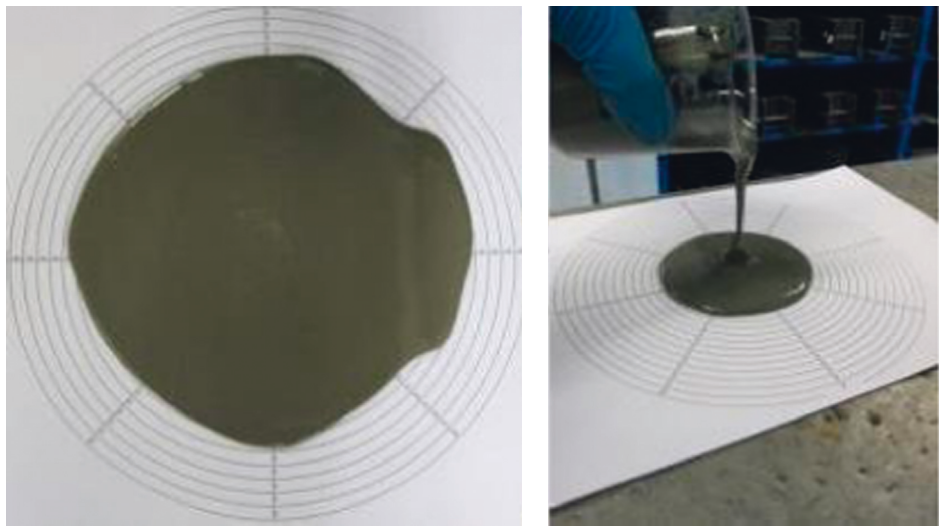

(a) (b)

Figure 1: Slump-flow measurement (a) and pouring of the cementitious matrix (b).

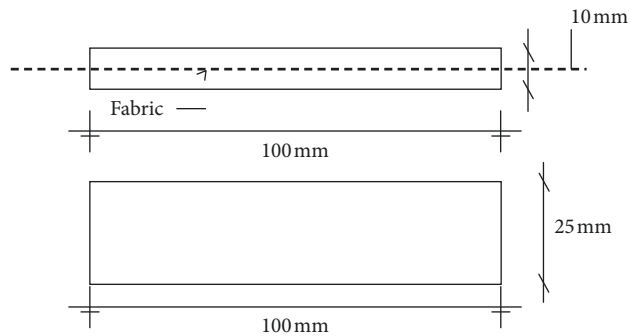

Figure 2: Fabric-reinforced concrete specimen dimensions.

Pullout tests of the fabric from the cementitious matrix were performed as shown in Figure 6. For each cementitious matrix composite, three test specimens were tested at a testing speed of 1 mm/min, providing an average result and standard deviation. The microstructure and cement paste penetration depth was determined using a field-emission scanning electron microscope (FESEM) type Quanta FEG 450 produced by FEI with an accelerating voltage set between 10 and 20 keV, a chamber pressure of 10–3 Pa, and a working distance of 15 mm. The back scattered electron (BSE) detector was used to obtain all images.

3. Results and Discussion

The workability of the produced UHPC mortars was determined only by measurements of the mini slump flow. The results showed an increased flow with an increasing W/B ratio (Figure 7). The measured compressive strength tended to decrease with a higher W/B ratio (Figure 8). The 7-day and the 28-day compressive strength values were nearly the same and within the calculated standard deviation. It can be related to the used steam curing which, as also shown earlier, resulted in a rapid early age strength development. The 7-day flexural strength increased from 12 MPa at the W/B ratio of

Figure 3: Formwork setup of fabric-reinforced test specimen.

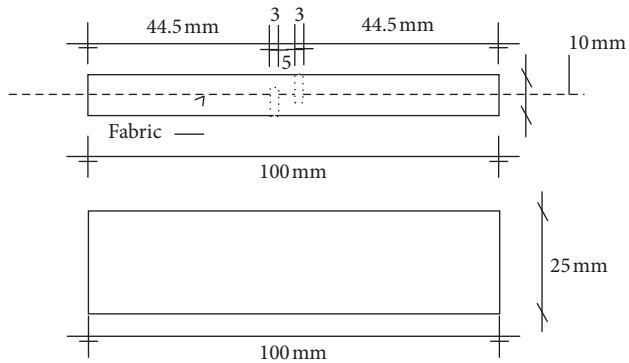

Figure 4: Specimen dimensions and configuration.

0.2 to nearly 15 MPa when the W/B ratio was 0.31. However, further increase of the W/B ratio to 0.33 caused a decrease of the flexural strength to 12 MPa. These values must be considered with a caution due to a relatively significant standard deviation of the measured values (Figure 8). The observed variations can be directly related to the entrapped air present despite the usage of the vacuum mixer. The negative effect of random small air voids was certainly enhanced by the small size of the used reference samples, $12 \times 12 \times 100\ \text{mm}^3$. Consequently, it can be assumed that the flexural strength was affected by the used W/B ratios only to a very limited extent, and the average value was 12 MPa after 7 days.

The pullout strength and the shear capacity of the study composites were determined on specimens made of the same mortars but incorporating additionally the glass fiber fabric (Figures 2–4). The measured single-lap shear strength increased with a decreasing W/B ratio (Figure 9). As shown and pointed by an arrow in Figure 5, mortars tended to form "mini beams" between the glass fiber bundles, connecting layers of mortars on both sides of the fabric. It was assumed that most of the shear stress was transferred through them and their mechanical properties defined the measured shear capacity of the composite. A higher measured shear capacity of composites using a lower W/B ratio could indicate a limited contribution of the bundles in this test setup. This assumption could explain a higher shear capacity of the composite despite a lower W/B ratio and thus worse penetration capacity. The results showed an opposite trend in the case of pullout strength. In this case, the measured maximum pullout forces were constant and reached around 3.3 kN/mm throughout the entire used W/B ratio range. The exception was the mix PR4 having the highest amount of water where the pullout strength increased to 4.5 N/mm (Figure 10). Certainly, a higher amount of water led to a lower viscosity of the fresh mix and thus to its better penetrability. The viscosity of the produced mortars appeared to be too low for a sufficient penetration between the single fibers until the W/B ratio was increased to 0.26, see also the SEM test results in Figure 11. The displacement versus the applied load was measured only on one sample (PR1) which had the W/B ratio of 0.2 (Figure 12). The results confirmed a typical pattern observed earlier [11]. In the first stage, when the maximum pullout force was reached, the measured displacement was around 0.5 mm. In the second stage, a decrease of the pullout force to just under 50 N was observed, followed by its slight increase and accompanied by a large displacement of up to 6 mm. The observed behavior is commonly known as a "telescopic failure" in which a successive layer by layer breakdown from the sleeve filaments to the core filaments occurs. Once the sleeve filaments fail in tension, the core filaments are pulled out of the yarn. The

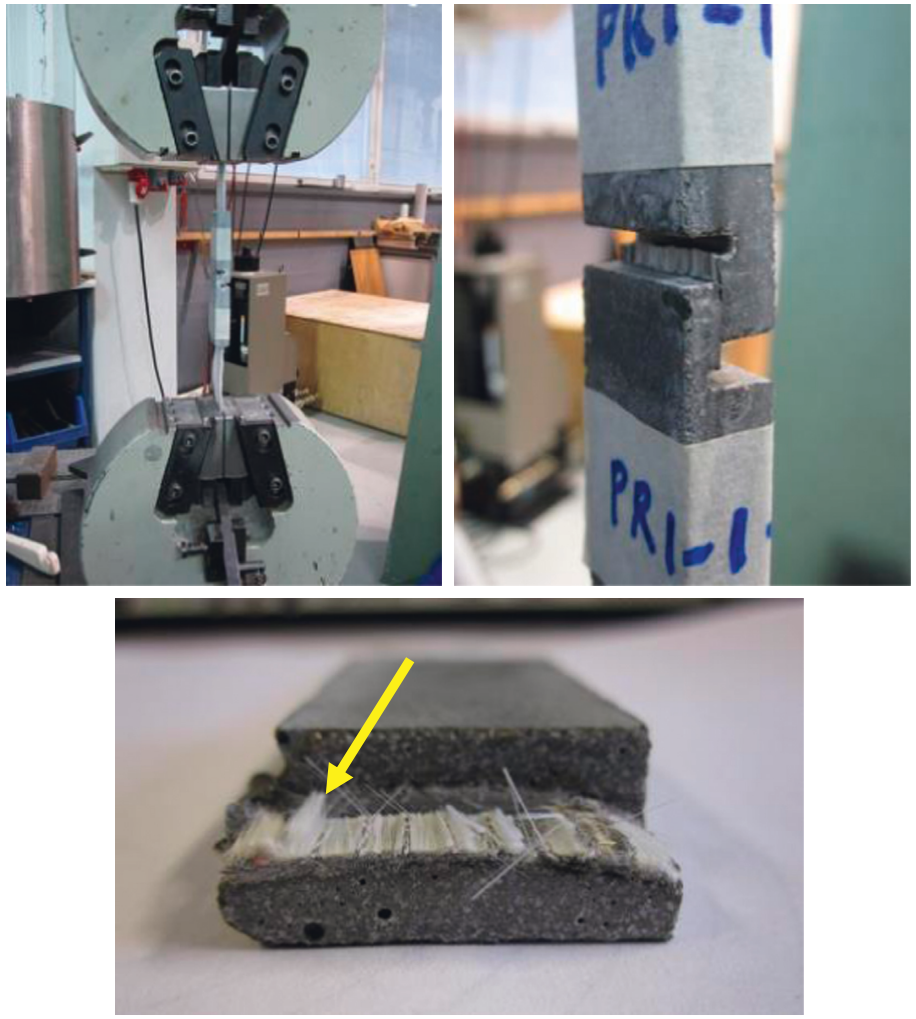

Figure 5: Single-lap shear strength test setup.

length of embedment of the yarn into the matrix has only a slight effect on the load-carrying capacity of the whole system [11, 12]. The maximum recorded load of 250 N is related to the failure of the sleeve filaments, while the second stage with a lower force but a large displacement is related to the progressive pullout and eventual failure of the core filament. The penetration depth of the cement matrix in between the glass fibers determined the volume of fibers, which are classified as a sleeve or a core in the load transfer. The higher the amount of the sleeve fibers, the higher the load bearing capacity of the entire system.

The penetration depth on the binder matrix between the single fibers was determined visually by analyzing SEM-BSE images of resin-impregnated and polished samples. Two extreme examples are shown in Figures 12 and 13. The penetration was deeper in the case of mixes having a higher water amount and thus a lower fresh state viscosity. In the case of a mix with a W/B ratio of 0.26, the penetration was estimated to reach up to 100 μm which created the sleeve filament to result in the highest recorded pullout strength (Figure 9). On the contrary, in the mix with the lowest W/B ratio of 0.2, almost no penetration between the single fibers was observed which also translated into a very low pullout strength value.

The main problem related to the penetration of mortars was the presence of fine particles including, in this case, quartz and sand. The particles even despite their very small diameter tended to be stopped by the closely spaced glass fibers, which formed an artificial sieve. Considering that a single glass fiber diameter is around 17 μm and the distance between fibers is much shorter, the maximum particle size should not exceed a few micrometers to enable their movement alongside the cement paste in between the fibers. The sieving effect is evidently visible in the studied samples where sand and quartz particles remained in the outer layer outside of the glass fiber bundle. The viscosity of the mortar and cohesive forces prevented extensive separation of the parts from the particles.

Several solutions could be used to improve the load capacity of UHPC glass fiber composites. The glass fiber fabric should be more loosely packed in comparison with the one used in these tests. The maximum particle size could be decreased to a few micrometers, thus enabling better penetration in between fibers.

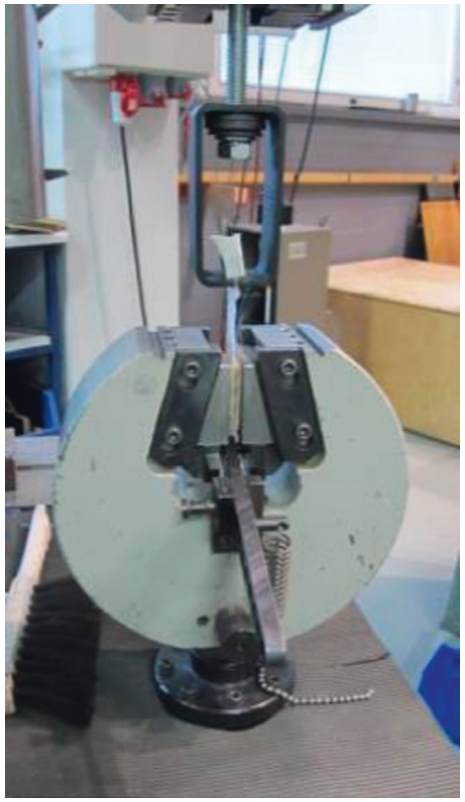

Figure 6: Test setup of pullout tests.

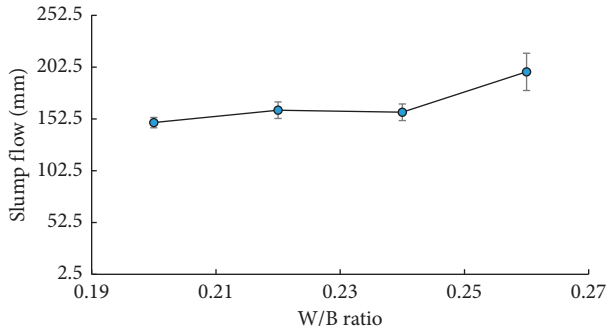

Figure 7: Measured slump flow.

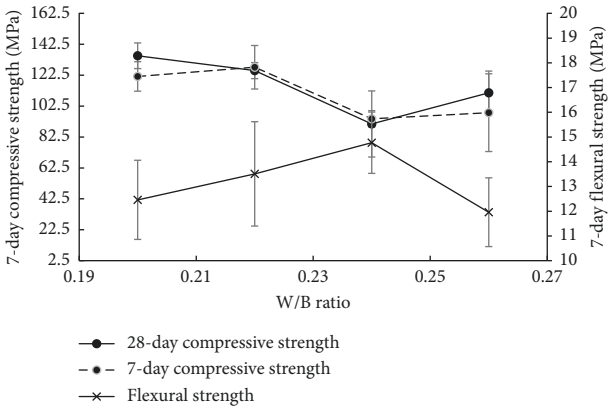

Figure 8: Flexural and compressive strength values versus water-to-binder ratio.

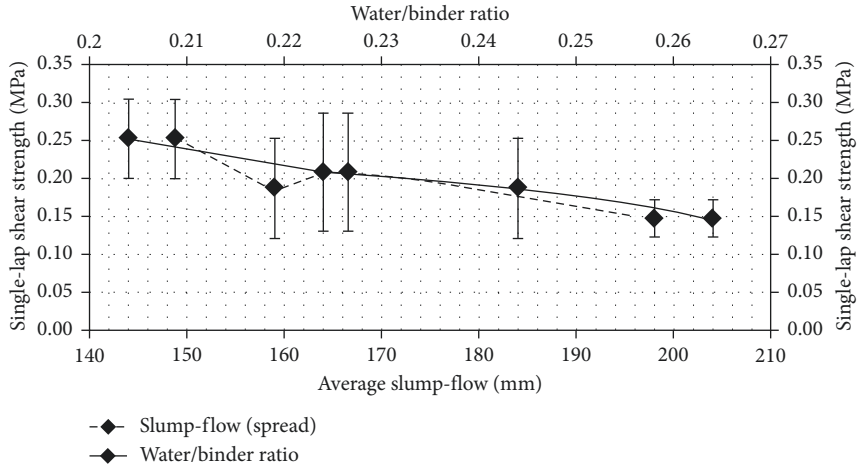

Figure 9: Single-lap shear strength versus average slump-flow and water/binder ratio.

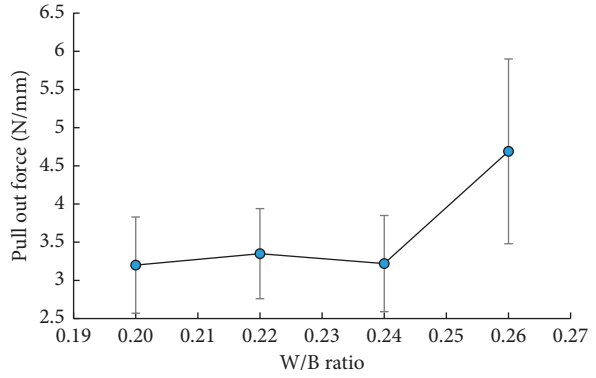

Figure 10: Pullout load versus water/binder ratio.

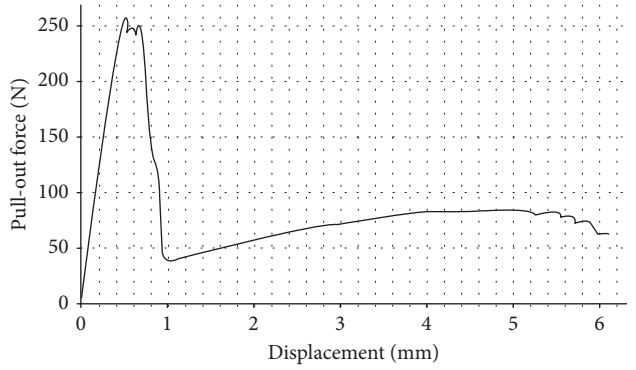

Figure 11: SEM images of sample PR5 (W/B = 0.2). No fibers imbedded into the binder matrix were observed.

4. Conclusions

The penetration depth of a low water-to-binder ratio mortar into a glass fiber fabric and its effects on selected mechanical properties were studied. The average penetration varied between 30 and 100 μm, depending on the used W/B ratio. The results showed that maximum particle size of quartz and sand should be below the average spacing of a single glass fiber. In the case of this study, the maximum particle size was estimated to be <20 μm. The compressive and the flexural strengths of the reference mortars reached 140 MPa and 15 MPa, respectively. The highest values were recorded for mortar with the lowest W/B ratio. The used experimental setup enabled also to determine the pullout force and the single lap shear strength of the mortar/glass fabric composites. The measured values reached 4.5 N/mm and 0.25 MPa, respectively. However, the highest pullout strength was obtained for the mortar having the highest W/B ratio while, on the contrary, the highest shear strength was measured for the mortar having the lowest W/B ratio. The

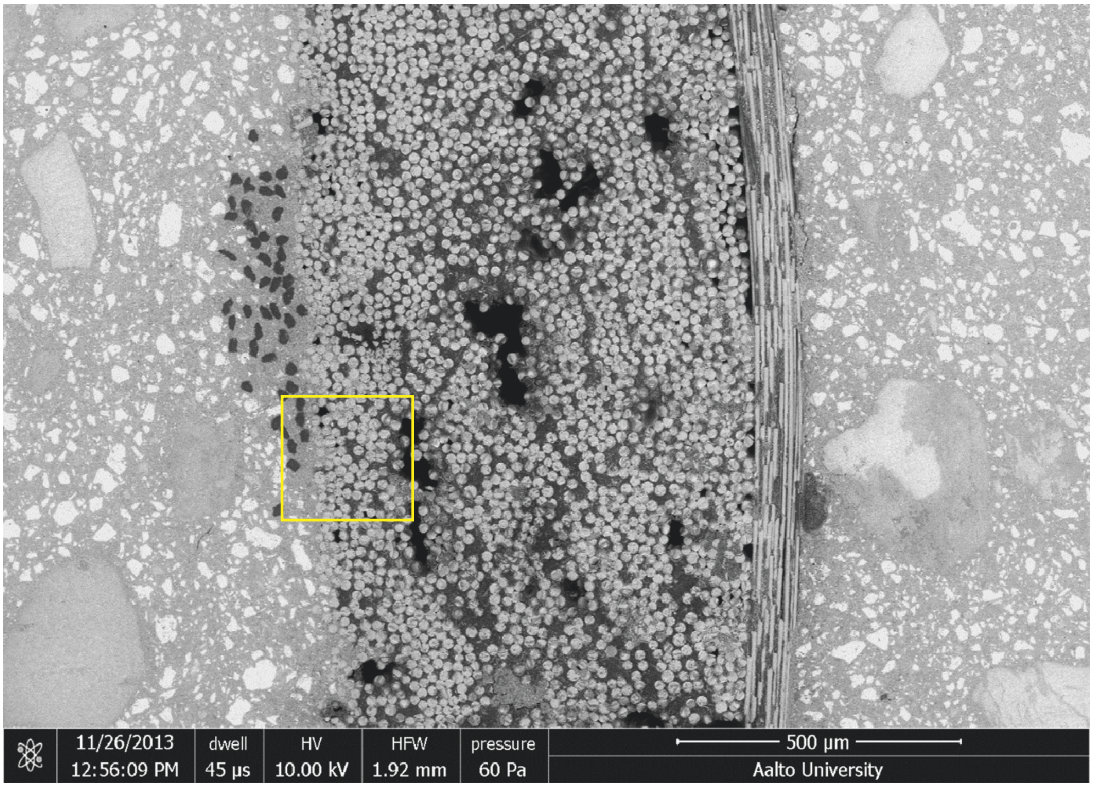

(a)

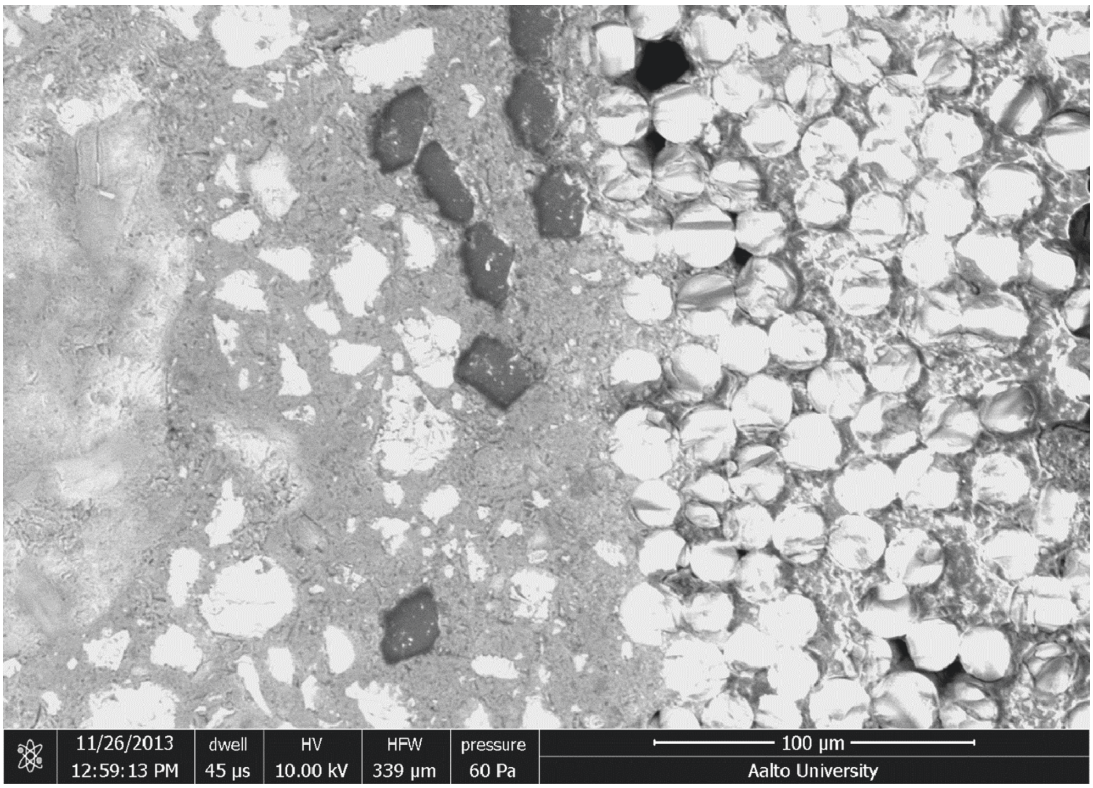

(b)

Figure 12: Displacement measured during the pullout test for mix PR1.

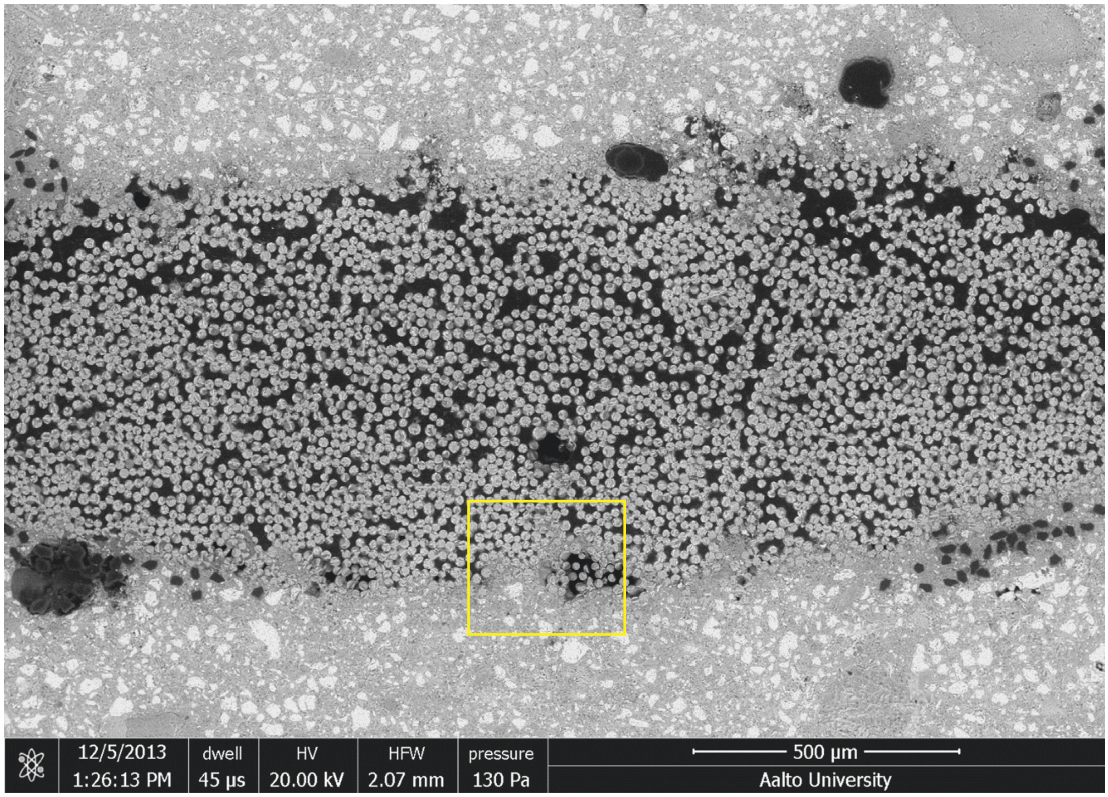

(a)

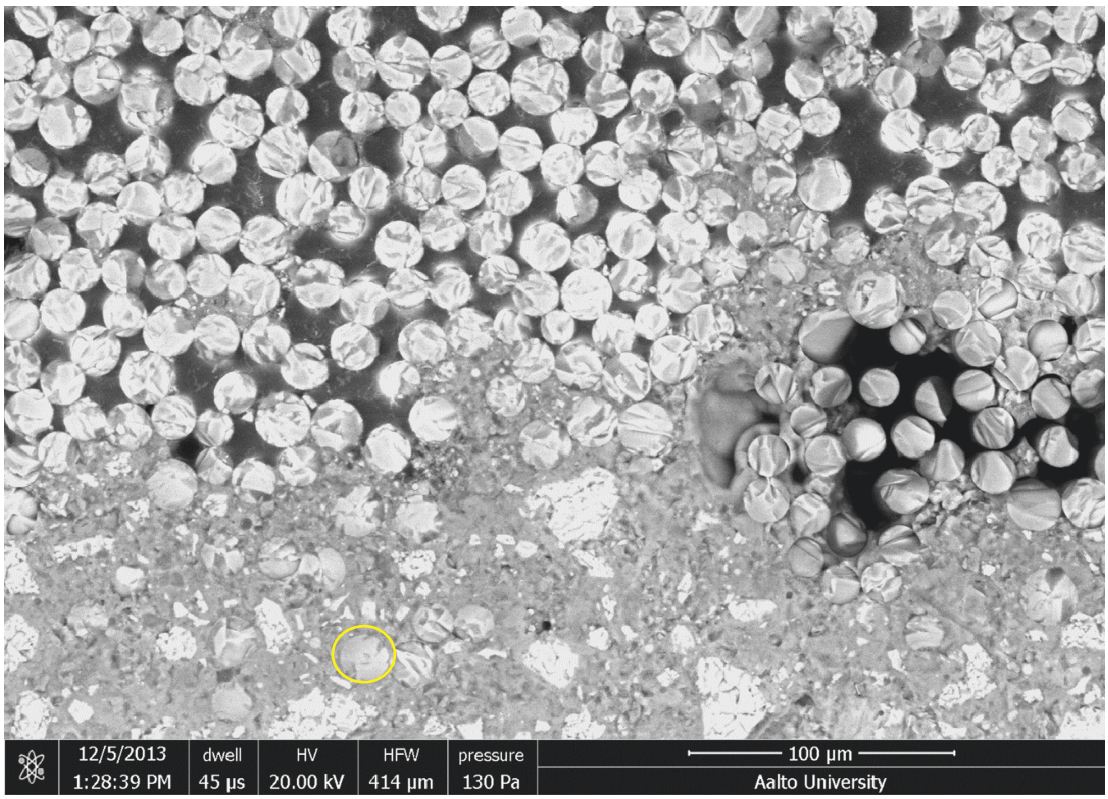

(b)

Figure 13: SEM images of samples PR6 (W/B = 0.26). A fiber fully imbedded into the binder matrix is marked in (b).

main reason was assumed to be related to the load transfer mechanism. In this case, the lap shear was mostly affected by the mortar filling in the volume between the fiber bundles. While, in the case of the pullout force, the penetration depth in between the single fibers appeared to be the most influential factor.

Data Availability

The data used to support the findings of this study are available from the corresponding author upon request.

Conflicts of Interest

The authors declare that they have no conflicts of interest.

References

[1] B. Brunauer, M. M. Yudenfreund, I. Odler, and J. Skalny, "Hardened portland cement pasted pf low porosity, VI mechanism of the hydration processes," *Cement and Concrete Research*, vol. 3, no. 2, pp. 129–147, 1973.

[2] H. H. Bache, "Densified cement/ultra-fine particle-based materials," in *Proceedings of International Conference on Superplasticizers in Concrete*, p. 12, Ottawa, Canada, 1981.

[3] J. D. Birchall, A. J. Howard, and K. Kendall, "Flexural strength and porosity of cement," *Nature*, vol. 289, no. 5796, pp. 388–390, 1981.

[4] F. De Larrard, "Ultrafine particles for making of very high strength concrete," *Cement and Concrete Research*, vol. 19, no. 2, pp. 161–172, 1988.

[5] P. Richard and M. Cheryrezy, "Composition of reactive powder concrete," *Cement and Concrete Research*, vol. 25, no. 7, pp. 1501–1511, 1995.

[6] A. Ajdukiewicz, B. Kotala, and M. Węglorz, "Application of non-metallic fabrics as reinforcement in thin-walled precast concrete members," *Architecture Civil Engineering Environment*, vol. 2, no. 2, pp. 57–66, 2009.

[7] A. E. Naaman, "Evolution in ferrocement and thin reinforced cementitious composites," *Arabian Journal for Science and Engineering*, vol. 37, no. 2, pp. 421–441, 2012.

[8] J. Hartig and U. Häußler-Combe, "A model for the uniaxial tensile behavior of textile reinforced concrete (TRC) covering effects at the micro and meso scales," in *Proceedings of European Conference on Fracture—Fracture of Materials and Structures from Micro to Macro Scale*, D. Klingbeil, M. Vormwald, and K. G. Eulitz, Eds., p. 91, Deutscher Verband für Materialforschung und -prüfung e.V., Dresden, Germany, September 2010.

[9] I. G. Colombo, A. Magri, G. Zani, M. Colombo, and M. di Prisco, "Textile reinforced concrete: experimental investigation on design parameters," *Materials and Structures*, vol. 46, no. 11, pp. 1933–1951, 2013.

[10] N. Zhao, H. Rödel, C. Herzberg, S.-L. Gao, and S. Krzywinski, "Stitched glass/PP composite. Part I: tensile and impact properties," *Composites Part A: Applied Science and Manufacturing*, vol. 40, no. 6, pp. 635–643, 2009.

[11] B. Banholzer, *Bond behaviour of a multi-filament yarn embedded in a cementious matrix*, Ph.D. thesis, Institut für Bauforschung der RWTH Aachen, Aachen, Germany, 2004.

[12] B. Banholzer, T. Brockmann, and W. Brameshuber, "Material and bonding characteristics for dimensioning and modelling of textile reinforced concrete (TRC) elements," *Materials and Structures*, vol. 39, no. 8, pp. 749–763, 2006.